

SCIENTIFIC REPORTS



OPEN

Three-Dimensional Carbon Allotropes Comprising Phenyl Rings and Acetylenic Chains in $sp+sp^2$ Hybrid Networks

Received: 07 October 2015

Accepted: 14 March 2016

Published: 18 April 2016

Jian-Tao Wang¹, Changfeng Chen², Han-Dong Li³, Hiroshi Mizuseki⁴ & Yoshiyuki Kawazoe^{5,6}

We here identify by *ab initio* calculations a new type of three-dimensional (3D) carbon allotropes that consist of phenyl rings connected by linear acetylenic chains in $sp+sp^2$ bonding networks. These structures are constructed by inserting acetylenic or diacetylenic bonds into an all sp^2 -hybridized rhombohedral polybenzene lattice, and the resulting 3D phenylacetylene and phenyldiacetylene nets comprise a 12-atom and 18-atom rhombohedral primitive unit cells in the $R\bar{3}m$ symmetry, which are characterized as the 3D chiral crystalline modification of 2D graphyne and graphdiyne, respectively. Simulated phonon spectra reveal that these structures are dynamically stable. Electronic band calculations indicate that phenylacetylene is metallic, while phenyldiacetylene is a semiconductor with an indirect band gap of 0.58 eV. The present results establish a new type of carbon phases and offer insights into their outstanding structural and electronic properties.

The valence electrons of carbon atom are capable of forming sp^3 -, sp^2 - and sp -hybridized states that support four basic types of single, double, triple, and aromatic carbon-carbon bonds^{1–4}. These different bonding states in various compounds have a profound impact on a wide range of properties of carbon-based materials. At ambient conditions, graphite, which is structurally related to polycyclic benzenoid aromatic hydrocarbon, is the thermodynamically most stable carbon configuration. The polycyclic carbon atoms form a two-dimensional (2D) benzenoid sp^2 bonding network with a bond angle of 120° and a bond length of 0.142 nm. Diamond, which is related to polycyclic saturated hydrocarbon, is the second most stable allotrope of carbon with all the carbon atoms in a methane-like tetrahedral sp^3 bonding state with a bond angle of 109.5° and a bond length of 0.154 nm as in alkanes, forming a very rigid three-dimensional (3D) carbon network. Linear carbyne, which is related to polyene-like unsaturated hydrocarbon with alternating single and triple carbon-carbon bonds rather than a cumulene structure, forming the simplest one-dimensional (1D) carbon chain, and it has been recently synthesized⁴, despite its rather high energy of about 1 eV per atom above that of graphite.

Since the discovery of fullerenes⁵, nanotubes⁶, and graphene⁷, considerable theoretical and experimental efforts have been made to search and assess new potential carbon allotropes^{8–20}. Intriguing among them are the so-called graphyne and graphdiyne^{21–24}, which are constructed by replacing one-third of the C–C bonds in graphene sheet with acetylenic (–C≡C–) or diacetylenic (–C≡C–C≡C–) linkages. Analogously, graphyne nanotubes²⁵ and fullereneynes²⁶ are also proposed theoretically. Thus far, large-scale graphyne and graphdiyne films composed of $sp+sp^2$ hybrid network^{27–29} have been successfully synthesized under laboratory conditions. Motivated by $sp+sp^2$ -hybridized 2D carbon allotropes, an $sp+sp^3$ -hybridized 3D diamondyne was suggested by inserting triple yne-bonds into all the C–C bonds in cubic diamond^{30–32}. In addition, a new material termed

¹Beijing National Laboratory for Condensed Matter Physics, Institute of Physics, Chinese Academy of Sciences, Beijing 100190, China. ²Department of Physics and High Pressure Science and Engineering Center, University of Nevada, Las Vegas, Nevada 89154, USA. ³State Key Laboratory of Environmental Criteria and Risk Assessment, Chinese Research Academy of Environmental Sciences, Beijing 100012, China. ⁴Computational Science Research Center, Korea Institute of Science and Technology (KIST), Hwarangno 14-gil 5, Seongbuk-gu, Seoul 02792, Republic of Korea. ⁵New Industry Creation Hatchery Center, Tohoku University, Sendai 980-8579, Japan. ⁶Institute of Thermophysics, Siberian Branch of Russian Academy of Sciences, Novosibirsk 630090, Russia. Correspondence and requests for materials should be addressed to J.T.W. (email: wjt@aphy.iphy.ac.cn)

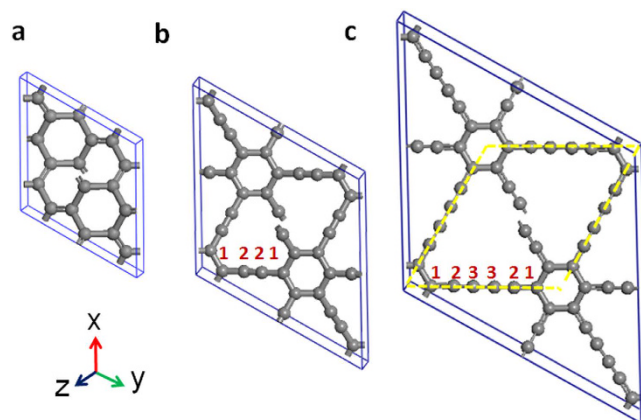


Figure 1. Three-dimensional carbon networks of rh6 polybenzene and polybenzene-ynes with phenylic rings and acetylenic chains in $R\bar{3}m (D_{3d}^5)$ symmetry. (a) Rh6 polybenzene in an all sp^2 3D bonding network with lattice parameters $a = 6.9022 \text{ \AA}$, $c = 3.470 \text{ \AA}$, occupying the 18h (0.8805, 0.1195, 0.5576) position, which comprises three zigzag benzene rings as its building blocks. (b) Rh12 phenylacetylene with lattice parameters $a = 11.6050 \text{ \AA}$ and $c = 3.6443 \text{ \AA}$. The 18h1 (0.8579, 0.9289, 0.4849) atoms form three benzene rings and 18h2 (0.8617, 0.7233, 0.6021) atoms form nine acetylenic yne-bonds located between the benzene rings. (c) Rh18 phenyldiacetylene with lattice parameters $a = 16.0963 \text{ \AA}$ and $c = 4.1987 \text{ \AA}$. The atoms on 18h1 (0.1023, 0.0511, 0.5065) site form three benzene rings; The atoms on 18h2 (0.1008, 0.8992, 0.4507) and 18h3 (0.1435, 0.8565, 0.3755) sites form nine butadiyne located between the benzene rings. The primitive cell is marked by yellow lines.

porous aromatic frameworks (PAFs) via inserting rigid phenyl rings into all the C–C bonds of diamond was reported^{33–35}. These studies open a new approach to constructing 3D covalent carbon network structures.

In this work we report *ab initio* total-energy and phonon calculations^{36–41} that predict a new type of 3D carbon phases in $R\bar{3}m (D_{3d}^5)$ symmetry constructed by inserting linear acetylenic chains into an sp^2 -hybridized rh6 polybenzene lattice³. The resulting 3D network structures of phenylacetylene and phenyldiacetylene consist of benzene rings bonding together with acetylene or diacetylene, which topologically correspond to 2D graphyne and graphdiyne, respectively. They are energetically more favorable than the sp -hybridized 1D carbyne chains and the recently reported $sp+sp^3$ -hybridized 3D diamondyne, and they are all dynamically stable. Moreover, 3D-phenylacetylene is metallic and 3D-phenyldiacetylene is semiconductor with an indirect band gap of 0.58 eV, in contrast to the semimetallic nature of graphite. These results provide new insights for the development of novel carbon allotropes.

Results and Discussion

We first present the structural characterization of the simplest 3D phenylacetylene network constructed by inserting triple (–C≡C–) yne-bonds into the rh6 polybenzene lattice (see Fig. 1a), as well as the so-called 2D graphyne by inserting triple yne-bonds into an expanded graphene sheet²¹. This new carbon phase has a $R\bar{3}m (D_{3d}^5)$ symmetry as that of rh6 polybenzene³ and topologically corresponds to 2D γ -graphyne²⁴. In the hexagonal representation, it has a 36-atom hexagonal unit cell (see Fig. 1b) with lattice parameters $a = 11.6050 \text{ \AA}$, $c = 3.6443 \text{ \AA}$, occupying the 18h1 (0.8579, 0.9289, 0.4849) and 18h2 (0.8617, 0.7233, 0.6021) Wyckoff positions. The carbon atoms on the 18h1 sites form three benzene rings, as in rh6 carbon, with aromatic sp^2 hybridization, while the carbon atoms on the 18h2 sites form nine triple yne-bonds located between the benzene rings with an ethyne-type sp -hybridization. As in rh6 carbon³, this structure also can be regarded as a three-dimensional chiral crystalline modification of carbyne connected via zigzag benzene rings with alternating single, triple and aromatic carbon-carbon bonds. It contains three distinct carbon-carbon bond lengths, a longer bond of 1.433 Å (C_1 – C_1) in the benzene rings and two shorter bonds of 1.389 Å (C_1 – C_2) and 1.232 Å (C_2 – C_2) associated with the single and triple bond in carbyne chains, respectively. Meanwhile, there are three different bond angles, 171.13° for $\angle C_1$ – C_2 – C_2 along the carbyne chains, 119.39° for $\angle C_1$ – C_1 – C_1 inside and 120.21° for $\angle C_1$ – C_1 – C_2 out of the zigzag benzene rings, respectively. On the other hand, in the rhombohedral representation, it has a 12-atom primitive unit cell with equilibrium lattice parameters $a = 6.8094 \text{ \AA}$, $\alpha = 116.889^\circ$, occupying the 6h (0.3428, 0.5560, 0.5560) and 6h (0.4638, 0.4638, 0.8788) position, thus this 3D-phenylacetylene is also termed as rh12 carbon.

The construction of 3D-phenylacetylene can also be applied to design a 3D-phenyldiacetylene network (see Fig. 1c) by inserting butadiyne (–C≡C–C≡C–) segments between the benzene rings in the rh6 polybenzene lattice. The resulting structure has a 54-atom hexagonal unit cell with an equilibrium lattice parameters $a = 16.0963 \text{ \AA}$, $c = 4.1987 \text{ \AA}$, occupying the 18h1 (0.1023, 0.0511, 0.5065), 18h2 (0.1008, 0.8992, 0.4507), and 18h3 (0.1435, 0.8565, 0.3755) Wyckoff positions. The carbon atoms on the 18h1 sites form three benzene rings, while the carbon atoms on the 18h2 and 18h3 sites form nine diyne-bonds. This 3D network structure has a $R\bar{3}m$ symmetry as in rh6 carbon, and topologically corresponds to 2D graphdiyne²⁴, thus there are four distinct carbon-carbon bond lengths, a longer bond of 1.427 Å (C_1 – C_1) is associated with the carbon atoms in the benzene rings and three shorter bonds of 1.395 Å (C_1 – C_2), 1.233 Å (C_2 – C_3), and 1.338 Å (C_3 – C_3) are along the chains

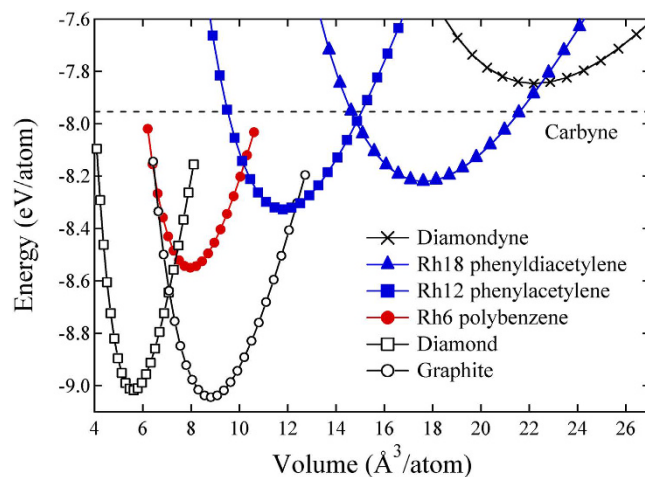


Figure 2. Energy versus volume per atom. Results for rh12 phenylacetylene and rh18 phenyldiacetylene compared to those of diamondyne, rh6 polybenzene, graphite and diamond. The dashed line indicates the energy level of 1D carbyne chain.

Structure	Method	$V_0(\text{Å}^3/\text{atom})$	a (Å)	c (Å)	d_{C-C} (Å)	E_{tot} (eV)	B_0 (GPa)	E_g (eV)
Diamond	LDA-LAA	5.604	3.552		1.538	-9.018	451	5.36
	Exp ⁴³	5.673	3.567		1.544		446	5.47
Rh6 polybenzene	LDA-LAA	7.968	6.9022	3.470	1.359, 1.483	-8.550	299	0.47
Rh12 phenylacetylene	LDA-LAA	11.81	11.605	3.644	1.232–1.433	-8.327	195	
Rh18 phenyldiacetylene	LDA-LAA	17.45	16.096	4.199	1.233–1.427	-8.221	129	0.58
Graphite	LDA-LAA	8.813	2.462	6.710	1.422	-9.045	280	
	Exp ⁴³	8.783	2.460	6.704	1.420		286	

Table 1. Calculated equilibrium structural parameters (volume V_0 , lattice parameters a and c , bond lengths d_{C-C}), total energy E_{tot} , bulk modulus B_0 , and electronic band gap E_g for rh6 polybenzene, rh12 phenylacetylene, rh18 phenyldiacetylene, graphite, and diamond at zero pressure, compared to available experimental data⁴³.

between the benzene rings. Note that the carbon chains are not perfectly linear with the bond angles of 172.54° for $\angle C_1-C_2-C_3$ and 180° for $\angle C_2-C_3-C_4$. In the rhombohedral representation, it has an 18-atom primitive unit cell, thus it also termed as rh18 carbon. The two new structures introduced here represent a new type of carbon allotropes that consist of phenyl rings connected by linear acetylenic chains in $sp+sp^2$ bonding networks.

The total energies of rh12 phenylacetylene and rh18 phenyldiacetylene as a function of volume are shown in Fig. 2 in comparison with the results for diamond, graphite, rh6 carbon, carbyne, and diamondyne. Our calculated energetic data establish the stability sequence: diamondyne < carbyne < rh18 < rh12 < rh6. It is clearly seen that the rh12 and rh18 polybenzene-ynes are located between the energy range for rh6 carbon and carbyne, with an energy gain of about 0.07 eV per atom, while the diamondyne is out of the energy range, and even less favorable than carbyne.

By fitting the calculated total energy as a function of volume to Murnaghan's equation of state⁴², we obtain the bulk modulus (B_0) of rh12 and rh18 carbon as 195 and 129 GPa, respectively. The atomic densities are estimated to be 2.50, 1.69, and 1.14 g/cm³ for rh6, rh12, and rh18 carbon, respectively, which are considerably different from 3.51 g/cm³ for diamond and 2.27 g/cm³ for graphite. We can see that with increasing of the acetylenic chain length, the atomic density and bulk modulus are decreasing to a level even lower than those of graphite. The calculated equilibrium structural parameters, total energy, and bulk modulus for diamond, rh6 polybenzene, rh12-phenylacetylene, rh18-phenyldiacetylene, and graphite are listed in Table 1 and compared to available experimental data⁴³.

We next examine the dynamic stability of the 3D $sp+sp^2$ bonding networks by phonon mode analysis. Figure 3a shows the phonon band structures and density of state (DOS) for the 3D phenylacetylene. The obtained phonon eigenvalues can be explained well by considering the bonding nature of the phenyl and triple carbon-carbon bonds. The vibrational modes due to the triple yne-bond can be observed clearly around 2150 cm⁻¹ with the carbon-carbon bond length of 1.232 Å (C_2-C_2) and the vibrational modes due to the phenyl bonds are distributed around 1500 cm⁻¹ with the carbon-carbon bond length of 1.433 Å (C_1-C_1). The combination modes of phenyl and triple bonds of carbon atoms can be seen clearly below 730 cm⁻¹. No imaginary frequencies were observed throughout the entire phonon band structures, thus confirming the dynamic stability of the 3D-phenylacetylene. Meanwhile, there is a large phonon band gap in the frequency range of 1500

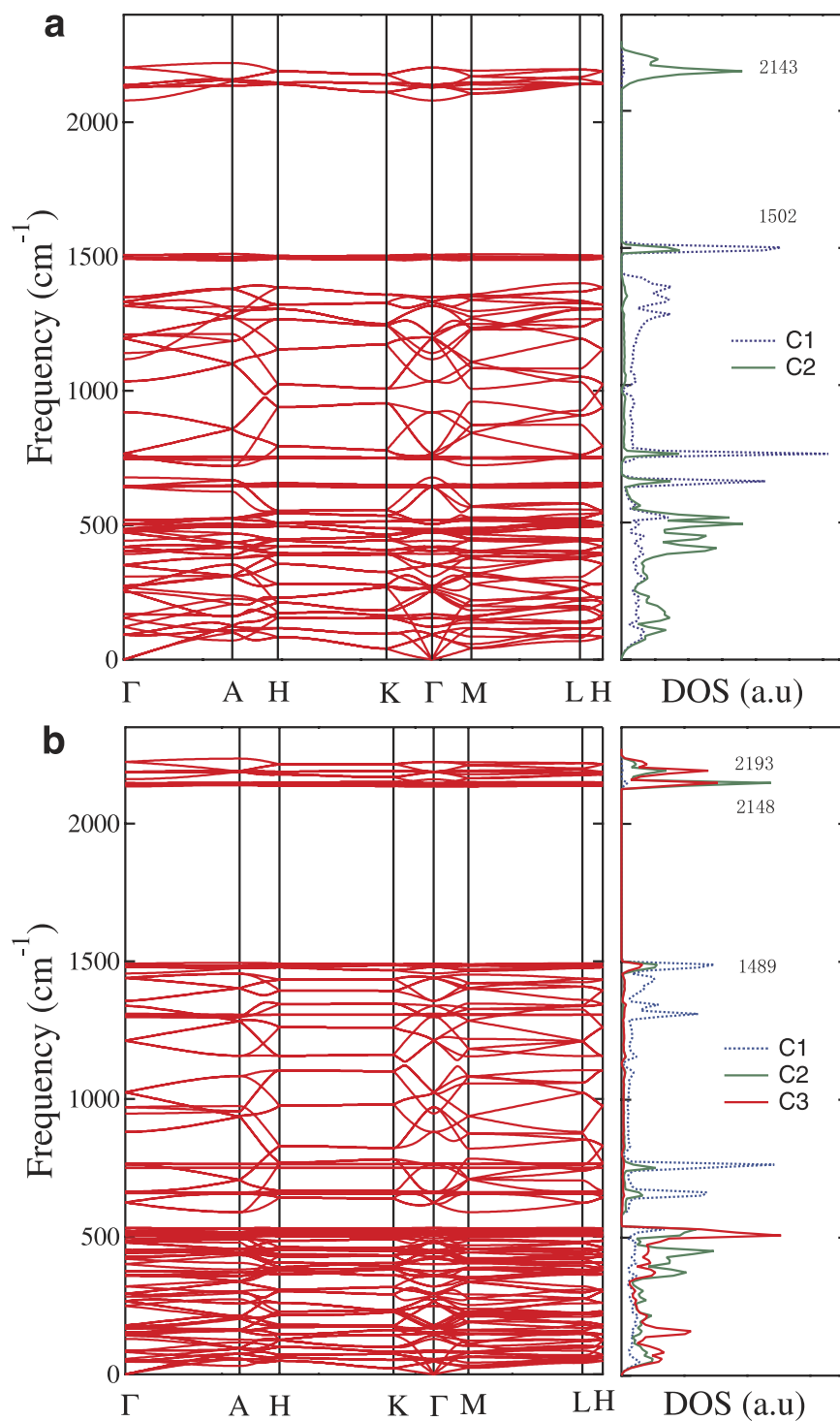


Figure 3. Phonon band structures and partial density of states (DOS). Results for rh12 phenylacetylene (a) and rh18 phenyldiacetylene (b). The spectra due to the triple bonds and phenyl bonds occur around 2150 cm^{-1} and 1500 cm^{-1} , respectively. A clearer picture for the low vibrational modes is given in Fig. S1 in Supplementary Information.

and 2100 cm^{-1} . Similar dynamic stability and vibrational modes are also confirmed for 3D phenyldiacetylene as shown in Fig. 3b. However, in the latter case there are two yne-modes around 2148 and 2193 cm^{-1} due to the diyne bonds related to the C_2 and C_3 carbon atoms.

To further examine the thermal stability, we have also performed *ab initio* molecular dynamics simulations using a $1 \times 1 \times 2$ hexagonal supercell, which contains 6 primitive cells. After being heated at room temperature (300 K) and 1000 K for 3 ps with a time step of 1 fs, no structural changes occurred for both rh12 and rh18 carbon. These results show that rh12 and rh18 carbon are viable carbon allotrope for experimental synthesis.

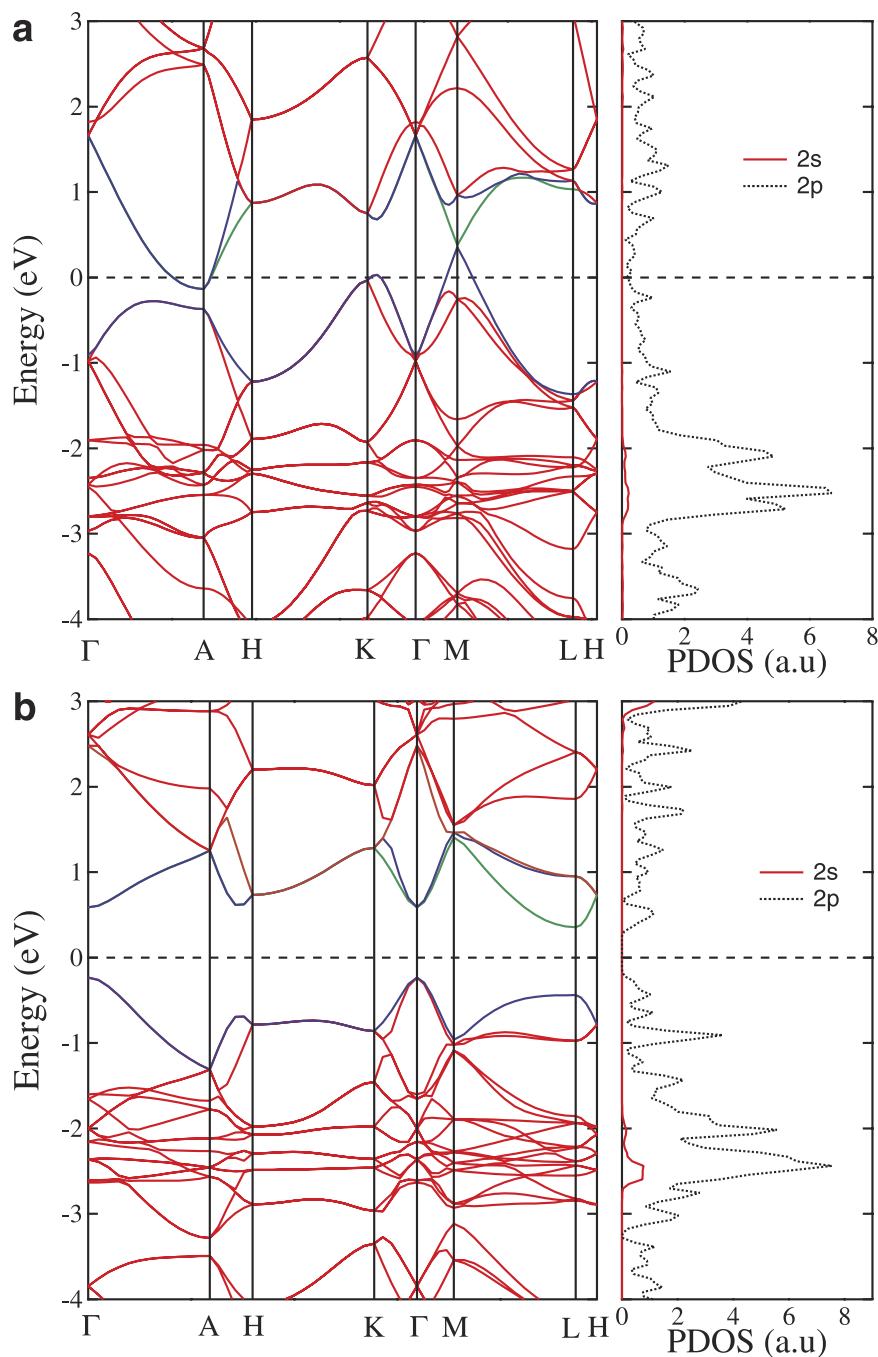


Figure 4. Electronic band structures and projected density of states (PDOS). Results for rh12 phenylacetylene (a) and rh18 phenyldiacetylene (b). The Fermi level is set at zero eV as indicated by the dashed lines.

Figure 4 shows the calculated electronic band structures and projected density of states (PDOS) by using the hybrid functionals (HSE06)³⁹. The calculated band gap for diamond is about 5.36 eV, which is closed to the experimental data of 5.47 eV⁴³, indicating the validity of the HSE06 method in predicting the band gaps for diamond and related sp^3 bonded carbon structures. For 3D-phenylacetylene, as shown in Fig. 4a, there are three bands around the A, K and M points across the Fermi level, resulting in the metallic nature of the system. Meanwhile, for 3D-phenyldiacetylene, as shown in Fig. 4b, the conduction band minimum and valence band maximum are located at the L and Γ point, respectively, showing a semiconductor character with an indirect band gap of 0.58 eV. Moreover, from the PDOS, we can see that the states around the Fermi level are mainly coming from the 2p orbitals, which define the metallic nature for phenylacetylene and the band gap for phenyldiacetylene.

To understand the bonding nature of electrons in both rh12 and rh18 carbon, the electron density difference (EDD) and electron localization function (ELF) maps are illustrated in Fig. 5. The EDD maps represent the variation of electron density in terms of chemical bonding. One can make an EDD plot by subtracting the overlapping

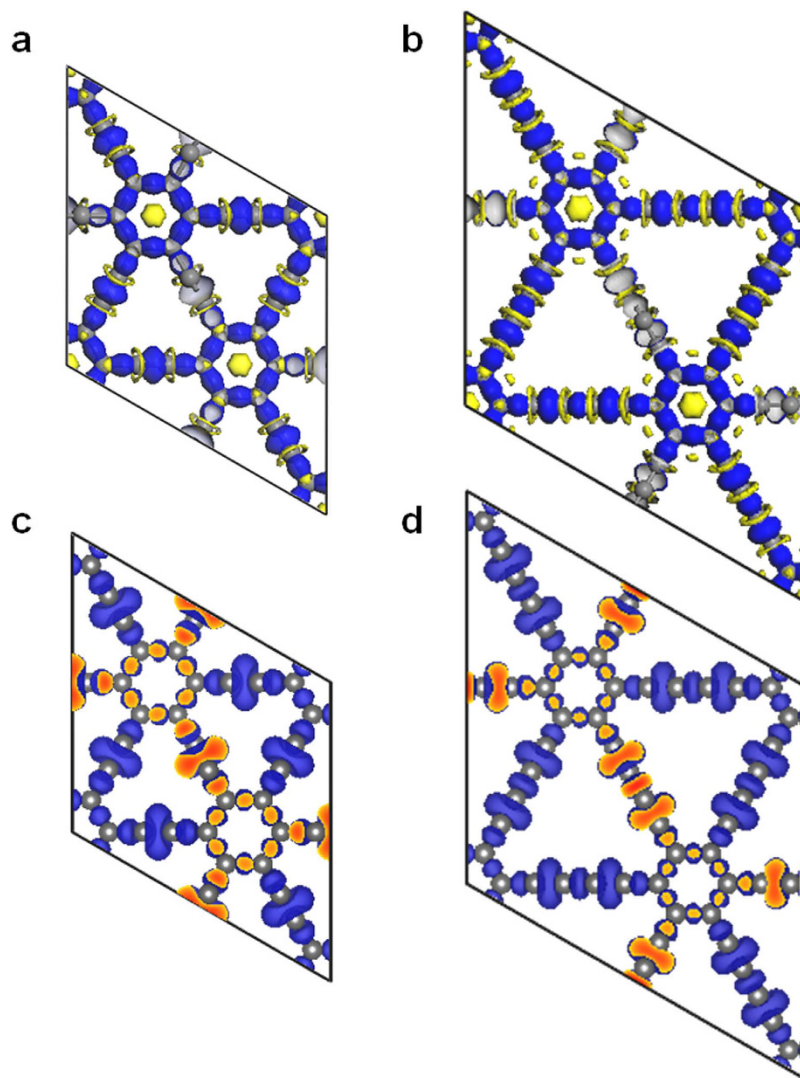


Figure 5. Electron density difference and electron localization function maps. (a,b) The electron density difference (EDD) for rh12 carbon (a) and rh18 carbon (b) with an isodensity of $0.1 \text{ e}/\text{\AA}^3$. The blue colour denotes a gain and the yellow colour a loss of electron density. (c,d) The electron localization function (ELF) for rh12 carbon (c) and rh18 carbon (d) with an isosurface level of 0.75.

atomic electron density from the self-consistent electron density of a crystal. The ELF maps can give a clear and quantitative description on the basic chemical bond (high ELF values $1 > \text{ELF} > 0.5$ indicate the formation of covalent bonds)^{44–46}, which was initially proposed by Becke and Edgecombe⁴⁵ based on Hartree-Fock theory, and generalized by Savin *et al.*⁴⁶ based on density functional theory. From the EDD maps shown in Fig. 5a,b, we can be seen that there is a larger gain of electron density between triple bonded carbons. Meanwhile, from the ELF maps shown in Fig. 5c,d, we can see that the electrons are well localized along the carbon chain, and the enhanced localization between triple bonded carbons can be seen clearly, which is more than the localization between the single and aromatic bonded carbons. These results show the strong triple bonding nature in the $sp+sp^2$ hybrid networks. Furthermore, to understand the aromaticity in the phenyl rings, the nuclear-independent chemical shift NICS(0) at the center of the phenyl rings are calculated using the gauge-including atomic orbital (GIAO) method at the B3LYP/6-311 + G(d,p) level⁴⁷. The NICS(0) values are estimated to be -8.16 ppm for benzene, -5.23 ppm for rh12 carbon, and -6.57 ppm for rh18 carbon. These results show that the aromaticity in phenyl rings of rh12 and rh18 carbon are smaller than the aromaticity in benzene.

Finally, we plot in Fig. 6a simulated x-ray diffraction (XRD) patterns for graphite, diamond, rh6 polybenzene, rh12 phenylacetylene, rh18 phenyldiacetylene and fcc C_{60} , compared to the experimental data for chimney soot and detonation soot⁴⁸. It is shown that the main (101) peak at 30° for rh6 should shift to 26° for rh12 and 22.4° for rh18 carbon. The main (101) peak at 26° for rh12 is very close to the main (002) peak at 26.5° for graphite, thus rh12 carbon may coexist with graphite in the detonation soot (see Fig. 6b and the Fig. 2 in ref. 48). On the other hand, for chimney soot, as shown in Fig. 6b, there is a sharp peak at 29.8° , which is fit well by the rh6 (101) diffraction peak, while a broad diffraction around 23° , which matches the rh18 (101) diffraction peak. These

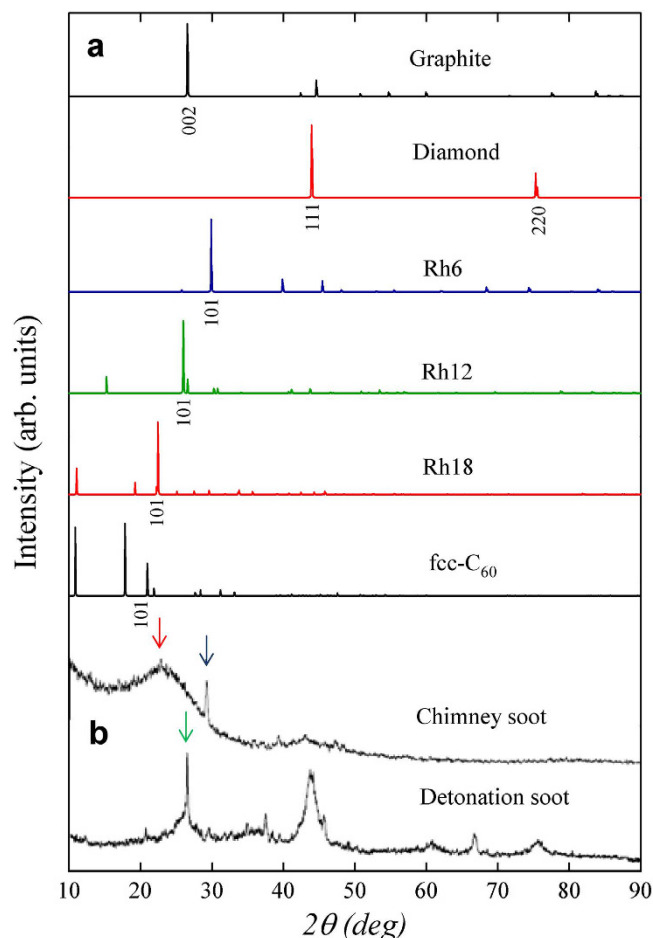


Figure 6. X-ray diffraction (XRD) patterns. (a) Simulated XRD patterns for graphite, diamond, rh6 polybenzene, rh12 phenylacetylene, rh18 phenyldiacetylene, and fcc C₆₀. (b) Experimental XRD patterns for chimney soot and detonation soot⁴⁸. The black, green, and red arrows indicate the XRD peaks corresponding to the main peak for rh6, rh12, and rh18 carbon, respectively. X-ray wavelength is 1.5406 Å with a copper source.

results suggest that rh12 and rh18 carbon as well as rh6 carbon may be present in chimney soot, carbon black or detonation soot⁴⁸.

Conclusions

In conclusion, we have identified by *ab initio* calculations a new type of three-dimensional carbon allotropes that consist of phenyl rings connected by linear acetylenic chains in $sp+sp^2$ bonding networks. The resulting 3D phenylacetylene and phenyldiacetylene network structures in $R\bar{3}m$ (D_{3d}^5) symmetry are topologically corresponding to 2D graphyne and graphdiyne, respectively, and they are energetically more favorable than the sp -hybridized 1D carbyne chains and the recently reported $sp+sp^3$ -hybridized 3D diamondyne. Phonon calculations show that these newly predicted structures are all dynamically stable. Electronic band and density of states calculations indicate that 3D-phenylacetylene with acetylenic yne-bonds is metallic, while 3D-phenyldiacetylene with diacetylenic yne-bonds is a semiconductor with an indirect band gap of 0.58 eV. Moreover, a detailed XRD analysis shows that phenylacetylene and phenyldiacetylene 3D network structures as well as rh6 polybenzene match the experimental diffraction peaks seen in the carbon black, diesel soot or chimney soot⁴⁸. Our findings suggest a novel strategy in constructing carbon framework structures that may help solve the structures of the newly discovered but unidentified carbon phases seen in recent detonation experiments.

Methods

Our calculations are carried out using the density functional theory as implemented in the Vienna *ab initio* simulation package (VASP)³⁶. The generalized gradient approximation (GGA) developed by Armiento-Mattsson (AM05)³⁷ were adopted for the exchange-correlation potential. The all-electron projector augmented wave (PAW) method³⁸ was adopted with $2s^22p^2$ treated as valence electrons. A plane-wave basis set with a large energy cut-off of 800 eV was used. Forces on the ions are calculated through the Hellmann-Feynman theorem allowing a full geometry optimization. The energy minimization is done over the atomic and electronic degrees of freedom using the conjugate gradient iterative technique. Convergence criteria employed for both the electronic self-consistent relaxation and the ionic relaxation were set to 10^{-8} eV and 0.01 eV/Å for energy and force,

respectively. A hybrid density functional method based on the Heyd-Scuseria-Ernzerhof scheme (HSE06)³⁹ has been used to calculate electronic properties. Phonon calculations are performed using the phonopy code⁴⁰ based on the supercell approach⁴¹ with a (1 × 1 × 2) 72-atom hexagonal supercell for rh12 and a (1 × 1 × 2) 108-atom hexagonal supercell for rh18 carbon. *Ab initio* molecular dynamics simulations under constant temperature (300 K and 1000 K) and volume (NVT) were performed to check thermal stability with a time step of 1 fs up to 3 ps. The nuclear-independent chemical shift NICS(0) at the center of the phenyl rings are calculated using the gauge-including atomic orbital (GIAO) method at the B3LYP/6-311 + G(d,p) level⁴⁷ as implemented in Gaussian03.

References

1. Belenkov, E. A. & Greshnyakov, V. A. Classification of structural modifications of carbon. *Phys. Solid State* **55**, 1754–1764 (2013).
2. Wang, J. T., Chen, C. F. & Kawazoe, Y. New carbon allotropes with helical chains of complementary chirality connected by ethene-type π -conjugation. *Sci. Rep.* **3**, 3077, doi: 10.1038/srep03077 (2013).
3. Wang, J. T., Chen, C. F., Wang, E. G. & Kawazoe, Y. A new carbon allotrope with six-fold helical chains in all- sp^2 bonding networks. *Sci. Rep.* **4**, 4339, doi: 10.1038/srep04339 (2014).
4. Chalifoux, W. A. & Tykwinski, R. R. Synthesis of polyynes to model the sp -carbon allotrope carbyne. *Nature Chem.* **2**, 967–971 (2010).
5. Kroto, H. W., Heath, J. R., O'Brien, S. C., Curl, R. F. & Smalley, R. E. C₆₀: Buckminsterfullerene. *Nature* **318**, 162–163 (1985).
6. Iijima, S. Helical microtubules of graphitic carbon. *Nature* **354**, 56–58 (1991).
7. Novoselov, K. *et al.* Electric field effect in atomically thin carbon films. *Science* **306**, 666–669 (2004).
8. Diederich, F. Carbon scaffolding: building acetylenic all-carbon and carbon-rich compounds. *Science* **369**, 199–207 (1994).
9. Karfunkel, H. R. & Dresslert, T. New hypothetical carbon allotropes of remarkable stability estimated by modified neglect of diatomic overlap solid-state self-consistent field computations. *J. Am. Chem. Soc.* **114**, 2285–2288 (1992).
10. Mao, W. L. *et al.* Bonding changes in compressed superhard graphite. *Science* **302**, 425–427 (2003).
11. Sheng, X. L., Yan, Q. B., Ye, F., Zheng, Q. R. & Su, G. T-Carbon: A novel carbon allotrope. *Phys. Rev. Lett.* **106**, 155703, doi: 10.1103/PhysRevLett.106.155703 (2011).
12. Niu, H. Y. *et al.* Families of superhard crystalline carbon allotropes constructed via cold compression of graphite and nanotubes. *Phys. Rev. Lett.* **108**, 135501, doi: 10.1103/PhysRevLett.108.135501 (2012).
13. Li, Q. *et al.* Superhard monoclinic polymorph of carbon. *Phys. Rev. Lett.* **102**, 175506, doi: 10.1103/PhysRevLett.102.175506 (2009).
14. Wang, J. T., Chen, C. F. & Kawazoe, Y. Low-temperature phase transformation from graphite to sp^3 orthorhombic carbon. *Phys. Rev. Lett.* **106**, 075501, doi: 10.1103/PhysRevLett.106.075501 (2011).
15. Wang, J. T., Chen, C. F. & Kawazoe, Y. Mechanism for direct conversion of graphite to diamond. *Phys. Rev. B* **84**, 012102, doi: 10.1103/PhysRevB.84.012102 (2011).
16. Wang, J. T., Chen, C. F. & Kawazoe, Y. Orthorhombic carbon allotrope of compressed graphite: *Ab initio* calculations. *Phys. Rev. B* **85**, 033410, doi: 10.1103/PhysRevB.85.033410 (2012).
17. Wang, J. T., Chen, C. F. & Kawazoe, Y. Phase conversion from graphite toward a simple monoclinic sp^3 -carbon allotrope. *J. Chem. Phys.* **137**, 024502, doi: 10.1063/1.4732538 (2012).
18. Amsler, M. *et al.* Crystal structure of cold compressed graphite. *Phys. Rev. Lett.* **108**, 065501, doi: 10.1103/PhysRevLett.102.065501 (2012).
19. Zhao, Z. S. *et al.* Tetragonal allotrope of group 14 elements. *J. Am. Chem. Soc.* **134**, 12362–12365 (2012).
20. Niu, C. Y., Wang, X. Q. & Wang, J. T. K₆ carbon: A metallic carbon allotrope in sp^3 bonding networks. *J. Chem. Phys.* **140**, 054514, doi: 10.1063/1.4864109 (2014).
21. Baughman, R. H., Eckhardt, H. & Kertesz, M. Structure-property predictions for new planar forms of carbon: Layered phases containing sp^2 and sp atoms. *J. Chem. Phys.* **87**, 6687–6699 (1987).
22. Haley, M. M., Brand, S. C. & Pak, J. J. Carbon networks based on dehydrobenzoannulenes: Synthesis of graphdiyne substructures. *Angew. Chem. Int. Ed. Engl.* **36**, 836–838 (1997).
23. Kim, B. G. & Choi, H. J. Graphyne: Hexagonal network of carbon with versatile Dirac cones. *Phys. Rev. B* **86**, 115435, doi: 10.1103/PhysRevB.86.115435 (2012).
24. Narita, N., Nagai, S., Suzuki, S. & Nakao, K. Optimized geometries and electronic structures of graphyne and its family. *Phys. Rev. B* **58**, 11009–11014 (1998).
25. Coluci, V. R., Braga, S. F., Legoas, S. B., Galv, D. S. & Baughman, R. H. Families of carbon nanotubes: Graphyne-based nanotubes. *Phys. Rev. B* **68**, 035430, doi: 10.1103/PhysRevB.68.035430 (2003).
26. Baughman, R. H., Galvão, D. S., Cui, C., Wang, Y. & Tománek, D. Fullereneynes: a new family of porous fullerenes. *Chem. Phys. Lett.* **204**, 8–14 (1993).
27. Li, G. X. *et al.* Architecture of graphdiyne nanoscale films. *Chem. Commun.* **46**, 3256–3258 (2010).
28. Ivanovskii, A. L. Graphynes and graphdienes. *Prog. Sol. State Chem.* **41**, 1–19 (2013).
29. Kehoe, J. M. *et al.* Carbon networks based on dehydrobenzoannulenes. 3. Synthesis of graphyne substructures. *Org. Lett.* **2**, 969–972 (2000).
30. Hirsch, A. The era of carbon allotropes. *Nat. Mater.* **9**, 868–871 (2010).
31. Jo, J. Y. & Kim, B. G. Carbon allotropes with triple bond predicted by first-principle calculation: Triple bond modified diamond and T-carbon. *Phys. Rev. B* **86**, 075151, doi: 10.1103/PhysRevB.86.075151 (2012).
32. Huang, L., Xiang, Z. & Cao, D. A porous diamond carbon framework: a new carbon allotrope with extremely high gas adsorption and mechanical properties. *J. Mater. Chem. A* **1**, 3851–3855 (2013).
33. Ben, T. *et al.* Gas storage in porous aromatic frameworks (PAFs). *Energy Environ. Sci.* **4**, 3991–3999 (2011).
34. Ren, H. *et al.* Targeted synthesis of a 3D porous aromatic framework for selective sorption of benzene. *Chem. Comm.* **46**, 291–293 (2010).
35. Ben, T. *et al.* Targeted synthesis of a porous aromatic framework with high stability and exceptionally high surface area. *Angew. Chem., Int. Ed.* **48**, 9457–9460 (2009).
36. Kresse, G. & Furthmüller, J. Efficient iterative schemes for *ab initio* total-energy calculations using a plane-wave basis set. *Phys. Rev. B* **54**, 11169–11186 (1996).
37. Armiento, R. & Mattsson, A. E. Functional designed to include surface effects in self-consistent density functional theory. *Phys. Rev. B* **72**, 085108, doi: 10.1103/PhysRevB.72.085108 (2005).
38. Blöchl, P. E. Projector augmented-wave method. *Phys. Rev. B* **50**, 17953–17979 (1994).
39. Krukau, A. V., Vydrov, O. A., Izmaylov, A. F. & Scuseria, G. E. Influence of the exchange screening parameter on the performance of screened hybrid functionals. *J. Chem. Phys.* **125**, 224106, doi: 10.1063/1.2404663 (2006).
40. Togo, A., Oba, F. & Tanaka, I. First-principles calculations of the ferroelastic transition between rutile-type and CaCl₂-type SiO₂ at high pressures. *Phys. Rev. B* **78**, 134106, doi: 10.1103/PhysRevB.78.134106 (2008).
41. Parlinski, K., Li, Z. Q. & Kawazoe, Y. First-principles determination of the soft mode in cubic ZrO₂. *Phys. Rev. Lett.* **78**, 4063–4066 (1997).

42. Murnaghan, F. D. The compressibility of media under extreme pressures. *Proc. Nat. Acad. Sci. USA* **30**, 244–247 (1944).
43. Ocelli, F., Loubeyre, P. & Letoullec, R. Properties of diamond under hydrostatic pressures up to 140 GPa. *Nature Mater.* **2**, 151–154 (2003).
44. Silvi, B. & Savin, A. Classification of chemical bonds based on topological analysis of electron localization functions. *Nature* **371**, 683–686 (1994).
45. Becke, A. D. & Edgecombe, K. E. A simple measure of electron localization in atomic and molecular systems. *J. chem. Phys.* **92**, 5397–5403 (1990).
46. Savin, A. *et al.* Electron localization in solid-state structures of the elements: the diamond structure. *Angew. Chem. Int. Ed.* **31**, 187–188 (1992).
47. Lee, C., Yang, W. T. & Parr, R. G. Development of the Colle-Salvetti correlation-energy formula into a functional of the electron density. *Phys. Rev. B* **37**, 785–789 (1988).
48. Pantea, D., Brochu, S., Thiboutot, S., Ampleman, G. & Schol, G. A morphological investigation of soot produced by the detonation of munitions. *Chemosphere* **65**, 821–831 (2006).

Acknowledgements

This study was supported by the National Natural Science Foundation of China (Grant No. 11274356) and the Strategic Priority Research Program of the Chinese Academy of Sciences (Grant No. XDB07000000). C.F.C. acknowledges support by DOE under Cooperative Agreement No. DE-NA0001982. Y.K. acknowledges support by the Russian Megagrant Project No. 14.B25.31.0030. We are thankful to the crew of the Computational Center of the Institute of Physics, Chinese Academy of Sciences, for their support at the Supercomputing facilities.

Author Contributions

J.-T.W., C.F.C., H.-D.L., H.M. and Y.K. designed the study and wrote the paper; J.-T.W. carried out *ab initio* simulations; all authors discussed the results and contributed to the manuscript.

Additional Information

Supplementary information accompanies this paper at <http://www.nature.com/srep>

Competing financial interests: The authors declare no competing financial interests.

How to cite this article: Wang, J.-T. *et al.* Three-Dimensional Carbon Allotropes Comprising Phenyl Rings and Acetylenic Chains in $sp+sp^2$ Hybrid Networks. *Sci. Rep.* **6**, 24665; doi: 10.1038/srep24665 (2016).



This work is licensed under a Creative Commons Attribution 4.0 International License. The images or other third party material in this article are included in the article's Creative Commons license, unless indicated otherwise in the credit line; if the material is not included under the Creative Commons license, users will need to obtain permission from the license holder to reproduce the material. To view a copy of this license, visit <http://creativecommons.org/licenses/by/4.0/>